THE JOURNAL OF BIOLOGICAL CHEMISTRY VOL. 286, NO. 22, pp. 19589–19596, June 3, 2011

Heterotrimeric G_i Proteins Link Hedgehog Signaling to Activation of Rho Small GTPases to Promote Fibroblast Migration*[S]

Received for publication, October 26, 2010, and in revised form, March 20, 2011 Published, JBC Papers in Press, April 7, 2011, DOI 10.1074/jbc.M110.197111

Ariel H. Polizio[‡1], Pilar Chinchilla[‡1], Xiaole Chen[‡1], Sangbumn Kim[‡], David R. Manning[§], and Natalia A. Riobo[‡¶2]

From the [‡]Department of Biochemistry and Molecular Biology and [¶]Kimmel Cancer Center, Thomas Jefferson University, Philadelphia, Pennsylvania 19107 and the [§]Department of Pharmacology, University of Pennsylvania School of Medicine, Philadelphia, Pennsylvania 19104

Evidence supporting the functionality of Smoothened (SMO), an essential transducer in most pathways engaged by Hedgehog (Hh), as a G_i-coupled receptor contrasts with the lack of an apparently consistent requirement for G_i in Hh signal transduction. In the present study, we sought to evaluate the role of SMO-G_i coupling in fibroblast migration induced by Sonic Hedgehog (Shh). Our results demonstrate an absolute requirement for G_i in Shh-induced fibroblast migration. We found that Shh acutely stimulates the small Rho GTPases Rac1 and RhoA via SMO through a G_i protein- and PI3K-dependent mechanism, and that these are required for cell migration. These responses were independent of transcription by Gli and of the C-terminal domain of SMO, as we show using a combination of molecular and genetic tools. Our findings provide a mechanistic model for fibroblast migration in response to Shh and underscore the role of SMO-G_i coupling in non-canonical Hh signaling.

Concerted cell proliferation, migration and differentiation in response to Hedgehog (Hh) proteins are required for normal embryonic development and postnatal homeostasis (1). Lack of Hh signaling is embryonic lethal, whereas hyperactivation of the Hh pathway underlies oncogenic transformation and promotes tumor maintenance in a large spectrum of human cancers, including basal cell carcinoma of the skin, medulloblastoma, rhabdomyosarcoma, some forms of leukemia, and gastric, pancreatic, biliary tract, breast, prostate, and lung adenocarcinomas (2–5). A role for Hh signaling has been reported in metastasis (6–8).

The Hh family of secreted proteins, Sonic (Shh), Indian (Ihh), and Desert Hedgehog (Dhh), exerts its functions by binding to the 12-transmembrane (12-TM)[3] receptor Patched1 (Ptc1) and, in a restricted cell population, Patched2 (Ptc2). Binding of Hh proteins to Ptc1 results in derepression of the 7-TM protein Smoothened (SMO). Ptc1 is thought to inhibit the activity of SMO by preventing its accumulation in the primary cilium, a single immotile flagellar-like structure derived from the centrosome present in most cells during interphase and after cell cycle exit (9, 10). Translocation of SMO to the primary cilium by lateral diffusion from the plasma membrane in response to Hh is presumed to cause a conformational change resulting in stimulation of transcription by the Gli family of transcription factors (Gli1, Gli2, and Gli3) (11–13).

We demonstrated recently that SMO has the capacity to signal through heterotrimeric G proteins (14). We showed, using [^{35}S]GTPγS binding, that SMO can activate all members of the G_i family of G proteins and was highly selective in this regard. This property is required, in NIH 3T3 cells, for activation of Gli-dependent transcription by Shh as it is blocked by a *Bordetella pertussis* toxin (PTX) (14), which uncouples most members of the G_i family from 7-TM receptors. Whether G_i is required in all cell types for activation of Gli transcription factors, however, is unlikely given the paucity of data regarding PTX in this context. Expression of PTX in the developing neural tube failed to perturb the classical morphogenetic function of Shh (15); for example, in this instance, as neural progenitors express G_z, a PTX-resistant form of G_i, it is conceivable that G_z compensates for the inhibition of other G_i family isoforms.

Although the best characterized cellular responses to Hh involve Gli-dependent transcription and occur over the course of hours if not days, many cell types respond to Hh in a seemingly Gli-independent fashion (16). Examples of the so called "non-canonical" Hh signaling are fibroblast migration, endothelial cell tubulogenesis, and axon growth cone repulsion, all of which are underlined by cytoskeletal changes (17–19). Fibroblasts deficient in Gli2 and Gli3 migrate in response to Shh indistinguishably from wild type counterparts (17). Although these cells still express very low levels of Gli1, the absence of an effect of Gli2/Gli3 deficiency and the time frame of the response suggest that Shh-induced cell migration is independent of Gli transcriptional activity.

We demonstrated previously in human endothelial cells that Hh isoforms are capable of stimulating the monomeric G protein RhoA in a G_i-dependent manner (18). In the present study, we sought to investigate the mechanistic basis underlying Shh-induced fibroblast migration, in particular to establish the role

* This work was supported, in whole or in part, by National Institutes of Health Grant GM080396.
[S] The on-line version of this article (available at http://www.jbc.org) contains supplemental Fig. S1.
[1] These authors contributed equally to this study.
[2] To whom correspondence should be addressed: Thomas Jefferson University, Bluemle Life Science Building, Room 922, 233 S. 10th St., Philadelphia, PA 19107. Fax: 215-923-1098; E-mail: natalia.riobo@jefferson.edu.
[3] The abbreviations used are: TM, transmembrane; PTX, pertussis toxin; GTPγS, guanosine 5′-*O*-(thiotriphosphate); MEF, mouse embryonic fibroblasts; DMSO, dimethyl sulfoxide; MOI, multiplicity of infection; KAAD-cyclopamine, 3-keto-*N*-(aminoethyl-aminocaproyl-dihydrocinnamoyl) cyclopamine; Adv, adenovirus.

of coupling of SMO to G_i in this paradigm. Our results reveal a strict requirement for G_i and PI3K in Shh-induced fibroblast migration, which is mediated by the rapid stimulation of Rac1 and RhoA small GTPases. We show as well that activation of the monomeric GTPases by SMO does not require Gli transcriptional activity nor any other signal encoded by the cytoplasmic C-terminal tail of SMO. These results suggest that SMO initiates canonical and non-canonical responses to Hh stimulation via separate domains and that G_i proteins play a central role in non-canonical signaling by linking Hh signaling to small Rho GTPases.

EXPERIMENTAL PROCEDURES

Reagents—KAAD-cyclopamine, purmorphamine, and LY294002 were from EMD Biosciences (Madison, WI). Pertussis toxin was purchased from Sigma-Aldrich. Anti-RhoA (67B9) rabbit mAb was obtained from Cell Signaling Technology (Danvers, MA), anti-Rac mouse clone 23A8 Ab from Millipore (Billerica, MA), and anti-SMO E5 mAb was purchased from Santa Cruz Biotechnology (Santa Cruz, CA). Secondary anti-rabbit-HRP and anti-mouse-HRP antibodies were from Santa Cruz Biotechnology, and rhodamine-phalloidin was purchased from Molecular Probes (Eugene, OR). DMEM and FBS were from Mediatech, Inc. (Waltham, MA), and newborn calf serum was from Invitrogen.

Plasmids and Adenoviral Vectors—Mouse SMO-M2 (obtained from P. Beachy, Stanford University) was subcloned into the pcDNA3.1+ vector. A C-terminal deletion, SMO-M2 (1–551), was created by PCR amplification and recloning. SMO-M2-CLD (W549A,R550A) was constructed by site-directed mutagenesis of full-length SMO-M2 plasmid using the QuikChange kit (Agilent Technologies, Santa Clara, CA). The vector series pAX142, pAX142-RhoN19, and pAX142-RacN17 were a generous gift of Dr. Andrew Aplin (Thomas Jefferson University). All other plasmids were described previously (14).

GFP AdV particles were a gift of Dr. Wally Koch (Thomas Jefferson University). Gli3R-GFP AdV was generated by homologous recombination of pShuttle-Gli3R-GFP (a generous gift of Dr. Bradley Yoder, University of Alabama) with the AdV backbone following the Adeno-X kit's directions (Clontech, Mountain View, CA). AdV particles were amplified in AD-293 cells, and the titer was determined using the AdEasy Viral Titer kit (Agilent Technologies, Santa Clara, CA).

Synthesis and Purification of Hedgehog Proteins—Recombinant Shh ligand was synthesized and purified as described previously (20). Briefly, Shh was synthesized as CBP-fusion proteins in *Escherichia coli*, purified using a calmodulin-affinity column with elution achieved by calcium. The purified fusion protein (inactive) was then cleaved at a single enterokinase site to release the intact (active) protein, which was then separated from the CBP peptide and cleaned from endotoxin contamination using Detoxi-Gel purification columns (Pierce). The specific activity was estimated by ability to induce a Gli-luciferase reporter in Light II fibroblasts in comparison with 5 μM purmorphamine (20).

Cell Culture—NIH 3T3 cells and $Smo^{-/-}$ mouse embryonic fibroblasts (MEFs) (from Dr. James Chen, Stanford University) were cultured in DMEM supplemented with 10% FBS and 100 units/ml penicillin-streptomycin. $Ptc1^{+/-}$ and $Ptc1^{-/-}$ MEFs (from Dr. Matthew Scott, Stanford University) were cultured in DMEM with 10% newborn calf serum and 100 units/ml penicillin-streptomycin. All cells were maintained in a humidified 37 °C incubator at 5% CO_2.

For the rescue experiments in $SMO^{-/-}$ MEFs, cells were transfected with pcDNA, SmoM2, SmoM2-ΔC, or SmoM2-CLD plasmids using Fugene HD (Roche Diagnostic). Stably transfected cells were selected with 75 μg/ml geneticin.

Rac and Rho Pulldown Assays—The cellular levels of GTP-loaded (active) Rac1 and RhoA were determined using a GST fusion protein containing the p21-binding domain of p21-activated kinase and the Rho binding domain of rhotekin, respectively (21, 22). Briefly, NIH 3T3, $Ptc1^{+/-}$, and $Ptc1^{-/-}$ fibroblasts were plated on 5-cm culture dishes and, prior to attaining confluence, were starved 16 h. The cells were then incubated with Shh (5 min for Rac1 and 15 min for RhoA) and lysed in 25 mM HEPES, pH 7.5, 150 mM NaCl, 1% Nonidet P-40, 10 mM $MgCl_2$, 1 mM EDTA, and 2% glycerol, and the lysate was clarified by centrifugation at 12,000 × *g* for 10 min. A portion of the supernatant aliquot was retained for measurement of total Rac1 and RhoA, whereas the remaining supernatant was incubated for 1 h at 4 °C with p21-binding domain-GST or Rho binding domain of rhotekin-GST bound to GSH-Sepharose 4B beads (GE Healthcare). Beads were washed three times, and bound proteins were eluted with Laemmli buffer, separated in 12% SDS-polyacrylamide gels (Mini Protean II System, Bio-Rad), and transferred onto nitrocellulose membranes. For RhoA detection, membranes were blocked in 5% bovine serum albumin-TBST (20 mM Tris, 150 mM NaCl, pH 7.5, containing 0.1% Tween 20), washed three times with TBST, and incubated with anti-RhoA (67B9) rabbit mAb antibody (1:1000) overnight at 4 °C. For Rac1 detection, membranes were blocked in PBS containing 3% nonfat dry milk at room temperature for 1 h, followed by five washes with mQ water and overnight incubation with anti-Rac1 23A8 mAb (1:1000) at 4 °C. After three washes with TBST for RhoA and five washes with mQ water for Rac1, the membranes were incubated with HRP-conjugated secondary antibodies at room temperature for 2 h. After extensive washing, the membranes were developed using the Western Lightning-ECL reagent (PerkinElmer Life Sciences). Band intensities were quantified using the free NIH ImageJ software. Densitometric values were first normalized to total RhoA or total Rac1 levels and then expressed as fold differences over the control treatment. When inhibitors were used, they were added 45 min before Shh or purmorphamine treatment except for PTX, which was added overnight prior to treatment.

Semi-quantitative RT-PCR—Total RNA was isolated from cells using the RNeasy kit (Qiagen, Valencia, CA) as directed. cDNA was synthesized from 2 μg RNA using the SuperScriptIII System (Invitrogen) with hexa-random primers following the protocol provided by the manufacturer. One μl of cDNA were used for PCR using the following sequence-specific primers: Gli1-F, 5′-GGA CCTGCA GAC GGT TAT CC; Gli1-R, 5′-AGC CTC CTG GAG ATG TGC AT; Ptc1-F, 5′-CGA TGG AGT CCT TGCCTA CAA; Ptc1-R, 5′-CCA CCA GAC GCT GTT TAG TCA; S15-F, 5′-TTC CGC AAGTTC ACC TAC C; and S15-R, 5′-CGG GCC GGC CAT GCTTTA CG.

Wound Healing Assays—The cells were seeded in 12-well plates (pre-coated with 2% gelatin) and cultured in complete medium until confluent. At that point, medium were replaced by DMEM containing 0.5% FBS for 24 h. Inhibitors or vehicles were added during the last 12 h (PTX, 100 ng/ml) or 45 min (15 μM LY294002 or 0.5 μM KAAD-CP) before $t = 0$. At $t = 0$, cells were washed once with PBS, and a scratch was made with an Eppendorf P20 pipette tip. PBS was replaced immediately with DMEM containing 0.5% FBS without or with purified Shh (2.5 μg/ml) or purmorphamine (5 μM) with or without inhibitors. Pictures of four zones along the scratch were taken at $t = 0$ h and $t = 8$ h using a Nikon Eclipse TS100 inverted microscope. For each sample, five distance measurements (in μm) were taken at evenly spaced points along the scratch at $t = 0$ h and $t = 8$ h, and cell migration was expressed as the (mean $t = 8$ − mean $t = 0$) for each sample. Results were expressed as μm in 8 h or percentage relative to the control group.

Statistics—Experiments comparing two groups were analyzed by a paired Student's *t* test. Those experiments involving comparison of three or more groups were analyzed by one-way analysis of variance, followed by Tukey's multiple comparisons test using GraphPad Prism (version 5.0).

RESULTS

Sonic Hedgehog Promotes Fibroblast Migration in a Smoothened-dependent Manner—To determine whether the coupling of SMO to one or more members of the G_i family has a role in fibroblast migration, we wanted to first establish whether cell migration induced by Shh is strictly dependent on SMO, as other routes of Shh signaling exist (16, 18). To this end, we compared the effect of Shh with that of purmorphamine, a direct SMO agonist, on migration. We used two cell lines to confirm the results, immortalized $Ptc1^{+/-}$ MEFs and NIH 3T3 fibroblasts. The first, which were used as a matter of convenience, behave and respond similar to wild-type MEFs to Shh (Ref. 23 and see below). Both Shh and purmorphamine stimulated migration of the cells 2–2.5-fold as determined by scratch-wound healing assays (Fig. 1, *A* and *B*, and supplemental Fig. S1, *black bars*). The response to the two agonists is comparable with other promigratory stimuli for fibroblasts, for example PDGF-BB (24). Pretreatment of cells with an inverse agonist specific for SMO, KAAD-cyclopamine, which prevents activation of Gli-dependent transcription as well as stimulation of G_i proteins by SMO (14), completely blocked cell migration in response to both agonists (Fig. 1, *A* and *B*, and supplemental Fig. S1, *white bars*). The basal rate of migration was similar in KAAD-cyclopamine- and vehicle (DMSO)-treated cells. These data, obtained with immortalized fibroblasts, demonstrate that Shh- and purmorphamine-elicited migration requires SMO.

We also extended the studies to primary MEFs. Complete Ptc1 deficiency results in de-repressed constitutive activation of SMO and embryonic lethality between 9.5–10 days post coitum (25). Thus, we compared the basal migration rate of MEFs isolated from $Ptc1^{-/-}$ 8.5 days post coitum embryos and from their $Ptc1^{+/-}$ littermates. Spontaneous wound closure by $Ptc1^{-/-}$ MEFs was faster than that by $Ptc1^{+/-}$ cells, and addition of KAAD-cyclopamine reduced the migration rate to that of $Ptc1^{+/-}$ cells (Fig. 1, *C* and *D*), indicating that the faster rate

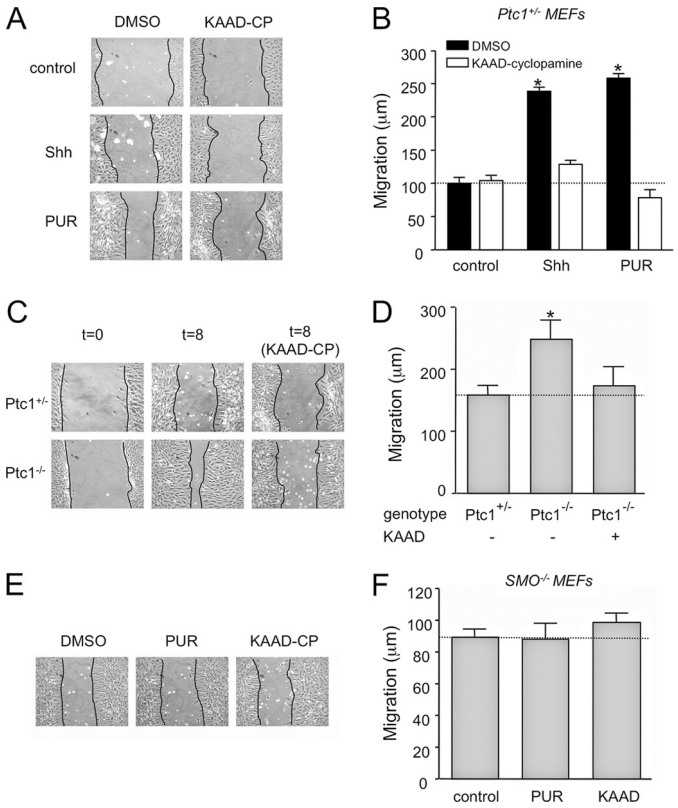

FIGURE 1. **Shh promotes fibroblast migration through SMO.** *A*, migration of $Ptc1^{+/-}$ mouse embryonic fibroblasts during 8 h after scratching a monolayer in the absence of serum. Vehicle (control) or 2.5 μg/ml Shh were added at $t = 0$ h. Photographs are representative of $n = 6$ experiments. *B*, quantification of $Ptc1^{+/-}$ migration without any stimulus (control), 2.5 μg/ml Shh (Shh), or 5 μM purmorphamine (*PUR*). Cells were pretreated with DMSO (*black bars*) or 0.5 μM KAAD-cyclopamine (*KAAD*) (*white bars*) ($n = 6$; *, $p < 0.001$). *C*, comparison of spontaneous migration of $Ptc1^{+/-}$ and $Ptc1^{-/-}$ MEFs in the absence or presence of 0.5 μM KAAD. *D*, quantification of basal $Ptc1^{+/-}$ and $Ptc1^{-/-}$ MEFs migration, the latter in the absence or presence of 0.5 μM KAAD ($n = 6$; *, $p = 0.023$). Representative images (*E*) and quantification (*F*) of wound healing assays using $SMO^{-/-}$ MEFs treated with 5 μM purmorphamine or 0.5 μM KAAD ($n = 6$).

is entirely attributable to constitutive SMO activation. The motility of MEFs deficient in SMO ($SMO^{-/-}$ MEFs, Fig. 1, *E* and *F*) was, as expected, far less than that of $Ptc1^{+/-}$ MEFs and insensitive to purmorphamine and KAAD-cyclopamine modulation. Altogether, the data confirm that Shh promotes fibroblast migration and establish that SMO is necessary and sufficient for this process.

Activation of PI3K/Akt and G_i Is Essential for SMO-induced Migration—Shh stimulates PI3K and Akt activities in fibroblasts and many other cells (26, 27). As shown in Fig. 2*A*, direct stimulation of SMO with purmorphamine increased Akt phosphorylation at Ser-473 in $Ptc1^{+/-}$ MEFs in a manner sensitive to KAAD-cyclopamine. Akt is often downstream of G_i and PI3K. To determine whether SMO promotes migration of fibroblasts via stimulation of G_i and/or PI3K, we pretreated $Ptc1^{+/-}$ MEFs with PTX or with LY294002, respectively. Both inhibitors completely blocked purmorphamine-stimulated migration (Fig. 2*B*).

We evaluated $Ptc1^{-/-}$ and $SMO^{-/-}$ MEFs as well. In $Ptc1^{-/-}$ MEFs, basal phosphorylation level of PDK-1 and Akt in the absence of serum was sensitive to inhibition by KAAD-

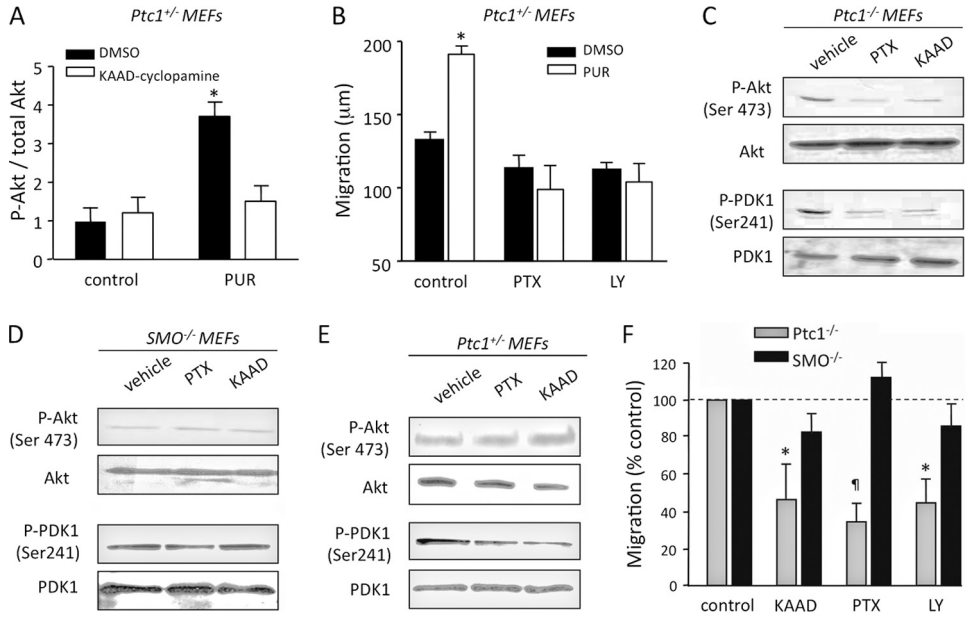

FIGURE 2. **SMO-dependent migration requires G_i and PI3K signaling.** *A*, serum-starved Ptc1$^{+/-}$ MEFs were stimulated for 15 min with 5 μM purmorphamine (*PUR*) or vehicle (control) in the absence or presence of 0.5 μM KAAD-cyclopamine. Whole cell lysates were separated by SDS-PAGE and blotted for P-Akt (Ser-473) and total Akt. Densitometry values of P-Akt (Ser-473) normalized to total Akt represent the mean ± S.E. of three experiments. *, $p < 0.05$. *B*, quantification of wound healing assays of Ptc1$^{+/-}$ MEFs pretreated with 100 ng/ml pertussis toxin or 15 μM LY294002 and stimulated with 5 μM purmorphamine or vehicle (DMSO) ($n = 6$; *, $p < 0.001$) *C–E*, representative experiment of P-Akt (Ser-473) and P-PDK1 (Ser-241) levels in serum-starved Ptc1$^{+/-}$ MEFs (*C*), SMO$^{-/-}$ MEFs (*D*), and Ptc1$^{-/-}$ MEFs (*E*) treated overnight with 100 ng/ml PTX or 0.5 μM KAAD-cyclopamine (KAAD) ($n = 3$). *F*, migration of Ptc1$^{-/-}$ MEFs (*gray bars*) or SMO$^{-/-}$ MEFs (*black bars*) in scratch-wound healing assays ($t = 8$ h) preincubated with 0.5 μM KAAD-cyclopamine (KAAD), 100 ng/ml PTX, or 15 μM LY294002 (*LY*). ($n = 4–6$; *, $p < 0.05$; ¶, $p < 0.01$).

cyclopamine and PTX (Fig. 2*C*). These data suggest that unconstrained activation of SMO in the absence of Ptc1 is able to maintain PI3K/Akt activation in a G_i-dependent manner. In SMO$^{-/-}$ MEFs, PDK-1 and Akt phosphorylation was not affected by KAAD-cyclopamine or PTX (Fig. 2*D*), as was the case in Ptc1$^{+/-}$ cells in the absence of Hh stimulation (Fig. 2*E*). Basal migration of Ptc1$^{-/-}$ MEFs was reduced by PTX and LY294002 (Fig. 2*F*, *gray bars*), comparable with the inhibitory effect of KAAD-cyclopamine. In contrast, SMO$^{-/-}$ MEFs migrated at a similar rate in the presence of vehicle, PTX, or LY294002 (Fig. 2*F*, *black bars*). These data confirm that the G_i/PI3K/Akt axis operates downstream of SMO to promote fibroblast migration.

Sonic Hedgehog Stimulates Small GTPases Rac1 and RhoA—Cell migration requires the coordinated activation of Rac and Rho, members of the Rho family of small GTPases. Shh might therefore regulate actin cytoskeleton dynamics through members of this family. To determine whether this is the case, we performed pulldown assays in NIH 3T3 cells stimulated with Shh. As shown in Fig. 3, *A* and *B*, Shh induced a biphasic activation of Rac1, with an early peak at 5 min and a later increase at 15 min. Shh also stimulated RhoA with a maximal effect between 5 and 10 min, which later led to a decline (Fig. 3, *C* and *D*). Moreover, migration of NIH 3T3 cells was dependent strictly on coordinated activation of Rac and Rho GTPases because expression of dominant negative RhoN19 or dominant negative RacN17 abrogated cell motility (Fig. 3, *E* and *F*). Exposure of Ptc1$^{+/-}$ MEFs to Shh also led to strong activation of both RhoA and Rac1 (Fig. 4), suggesting that this was not an exclusive feature of NIH 3T3 fibroblasts. Next, we reasoned that if Shh stimulates Rac1 and RhoA activity in a SMO-depen-

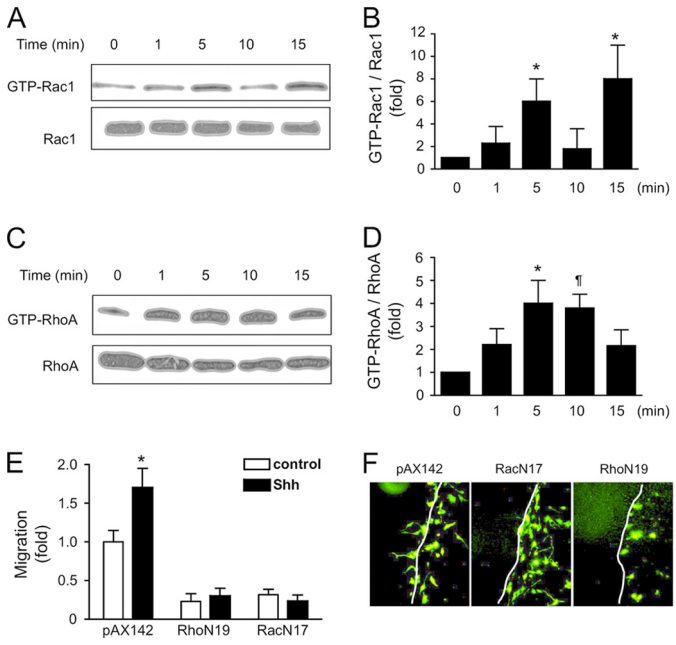

FIGURE 3. **Shh stimulates RhoA and Rac1 small GTPases.** *A*, representative Rac1 pulldown assay of serum-starved NIH 3T3 cells stimulated for 0–15 min with 2.5 μg/ml Shh. *B*, densitometry values of three independent time course Rac1 pulldown experiments. *, $p < 0.05$. *C*, representative RhoA pulldown assay of serum starved NIH 3T3 cells stimulated for 0–15 min with 2.5 μg/ml Shh. *D*, densitometry values of three independent time-course RhoA pulldown experiments; *, $p < 0.05$; ¶, $p < 0.01$. *E*, quantification of wound healing assays of NIH 3T3 cells co-transfected with GFP and pAX142 (empty vector), pAX142-RhoN19, or pAX142-RacN17 and stimulated at $t = 0$ with 2.5 μg/ml Shh or vehicle. Values represent the fold increase of GFP$^+$ cells that migrate into the wound. *, $p < 0.05$. *F*, representative images of migration of cells expressing pAX142, pAX142-RhoN19, or pAX142-RacN17 after 8 h in the presence of Shh. The *white line* shows the scratch border at $t = 0$. Note that green cells expressing pAX142-RhoN19 or pAX142-RacN17 are incapable of moving into the wound.

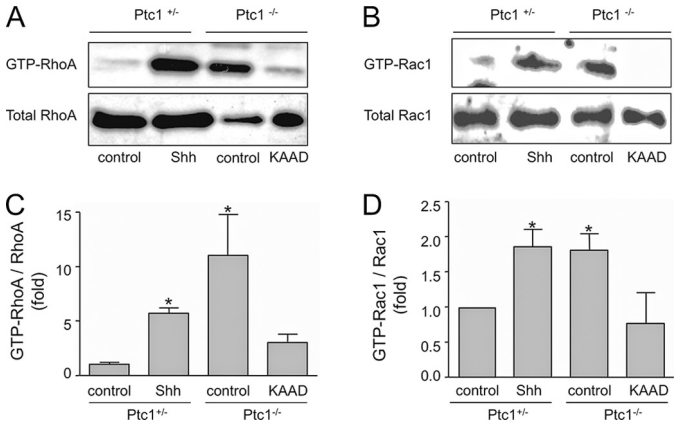

FIGURE 4. **Constitutive activation of SMO in Ptc1$_{-/-}$ MEFs leads to high basal RhoA and Rac1 activity.** *A*, Ptc1$^{+/-}$ cells were serum-starved for 24 h and stimulated with 2.5 μg/ml Shh or vehicle for 10 min. Ptc1$^{-/-}$ MEFs were serum-starved for 24 h and incubated during the last 45 min with vehicle or 0.5 μM KAAD-cyclopamine. The basal and stimulated levels of GTP-RhoA were determined by pulldown assays as described under "Experimental Procedures." *B*, GTP-Rac1 levels were evaluated by pulldown assays in conditions identical to *A*. Quantification of fractional RhoA (*C*) and Rac1 (*D*) GTP loading by densitometry ($n = 3$; *, $p < 0.05$).

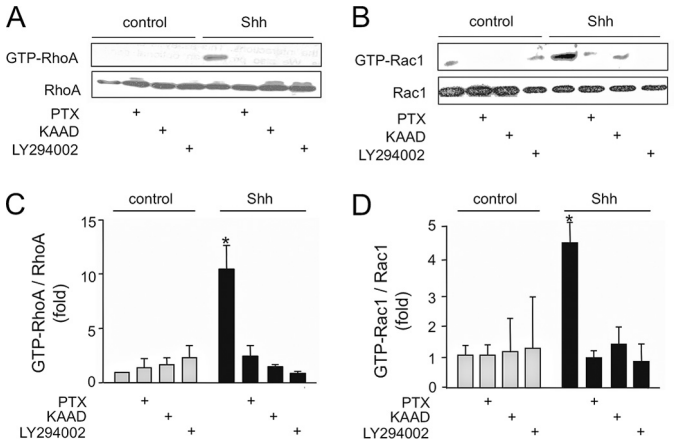

FIGURE 5. **Shh stimulates RhoA and Rac1 in a SMO-, G_i-, and PI3K-dependent manner.** *A*, representative RhoA pulldown assay of serum starved NIH 3T3 cells stimulated for 10 min with 2.5 μg/ml Shh and pretreated with vehicle, 100 ng/ml PTX, 0.5 μM KAAD-cyclopamine (KAAD), or with 15 μM LY294002. *B*, representative Rac1 pulldown assay of serum-starved NIH 3T3 cells stimulated for 5 min with 2.5 μg/ml Shh and pretreated as in *A*. *C*, densitometry values of three independent RhoA pulldown experiments. *, $p < 0.001$. *D*, densitometry values of three independent Rac1 pulldown experiments. *, $p < 0.05$.

dent manner, the high SMO activity in Ptc1$^{-/-}$ MEFs should be reflected in a high constitutive activation of those small GTPases. Indeed, Ptc1$^{-/-}$ MEFs showed an already high level of GTP-RhoA and GTP-Rac1 (Fig. 4), comparable with or higher than the Ptc1$^{+/-}$ cells stimulated with Shh. This increase in RhoA and Rac1 activity in Ptc1$^{-/-}$ MEFs is dependent on SMO because it was completely reduced to normal levels by pretreatment of the cells with KAAD-cyclopamine.

Because migration induced by Shh requires G_i and PI3K, we examined whether activation of Rac1 and RhoA is mediated by the same pathway. Pretreatment of NIH 3T3 cells with PTX and LY294002 blocked RhoA activation to a similar extent that KAAD-cyclopamine (Fig. 5, *A* and *C*). Shh stimulated Rac1-GTP loading was equally sensitive to LY294002, PTX, and KAAD-cyclopamine (Fig. 5, *B* and *D*).

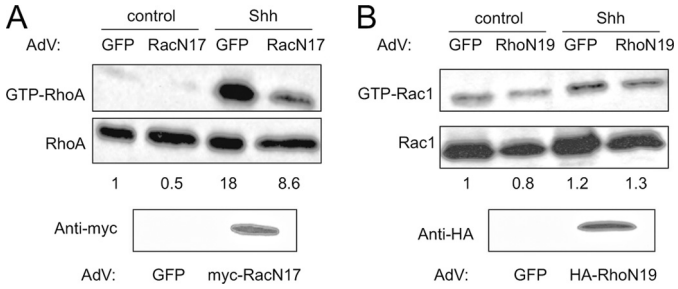

FIGURE 6. **Rac1 activity is required for full RhoA activation by Shh.** *A*, RhoA pulldown assay of Ptc1$^{+/-}$ MEFs transduced with control GFP-AdV or Myc-RacN17-AdV (MOI = 150) and stimulated with 2.5 μg/ml Shh or vehicle (control). Densitometry values of a representative experiment are shown *below* the gel. In the *bottom* gel, expression of RacN17 was confirmed by Western blot. *B*, Rac1 pulldown assay of Ptc1$^{+/-}$ MEFs transduced with control GFP-AdV or HA-RhoN19-AdV (MOI = 150) and stimulated with 2.5 μg/ml Shh or vehicle. Densitometry values of a representative experiment are shown *below* the gel. Expression of RhoN19 was confirmed by Western blot to the epitope tag (*bottom* gel).

Lastly, we evaluated whether activation of RhoA and Rac1 by G_i and PI3K are independent events or whether the activation of Rac is necessary for that of Rho. For this purpose, Ptc1$^{+/-}$ MEFs were transduced with a control GFP AdV or a dominant negative mutant RacN17 AdV at an MOI of 150 and, after 24 h, the cells were placed in serum-free medium. Addition of Shh elicited a robust activation of RhoA in GFP AdV-infected cells but an ~50% lower activation in RacN17-expressing cells (Fig. 6*A*), which correlates with an approximate 50% viral infection efficiency. In contrast, introduction of dominant negative Rho mutant (RhoN19) in Ptc1$^{+/-}$ MEFs did not perturb Rac1 activation when compared with GFP-expressing cells (Fig. 6*B*). These results suggest that the Shh-mediated activation of RhoA is at least partly dependent on Rac activity. Altogether, these findings reveal a novel mechanism linking SMO to small GTPases of the Rho family in fibroblasts, which is mediated by one or more members of the heterotrimeric G_i family and by PI3K.

Requirement for G_i Proteins Is Unrelated to Gli Transcriptional Activity—We reported previously that G_i is necessary for activation of Gli by Shh and by a mutant activated SMO in NIH 3T3 cells (14). Although the activation of Rac1 and RhoA by Shh seems too rapid to be a consequence of a transcriptional event, we wanted to rule out that PTX was inhibiting small GTPase activation by impairing Gli transcriptional activity. In contrast to our findings in NIH 3T3 cells, induction of the Gli target genes *gli1* and *ptc1* in Ptc1$^{+/-}$ MEFs in response to Shh or purmorphamine was not affected at all by treatment with PTX, as determined by RT-PCR or real-time PCR (Fig. 7, *A* and *B*). As a control, KAAD-cyclopamine completely prevented *gli1* and *ptc1* induction, and LY294002 had a significant inhibitory effect as well, as we described previously (26). The same was observed in primary MEFs (data not shown). Moreover, expression of *gli1* in unstimulated Ptc1$^{-/-}$ MEFs was high, consistent with constitutive SMO activity, and was also insensitive to PTX but sensitive to KAAD-cyclopamine and LY294002 (Fig. 7*C*). SMO$^{-/-}$ MEFs were used as a control for basal SMO-dependent *gli1* expression (Fig. 7*C*).

Because the insensitivity of Gli activation to PTX in MEFs was unexpected, we considered the possibility that they express

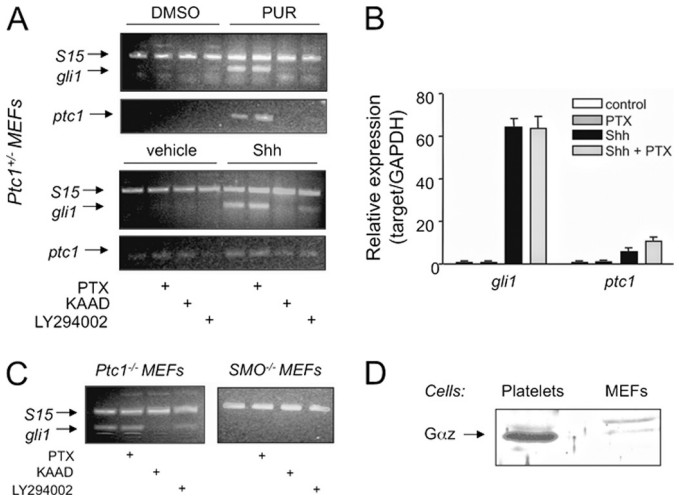

FIGURE 7. **Pertussis toxin does not affect Gli-dependent transcription in MEFs.** *A*, expression of *gli1*, *ptc1*, and the housekeeping gene *S15* was analyzed by semiquantitative RT-PCR. Ptc1$^{+/-}$ MEFs were grown until fully confluent, pretreated with 100 ng/ml PTX, 0.5 μM KAAD-cyclopamine, or 15 μM LY294002 and then stimulated with 2.5 μg/ml Shh, 5 μM purmorphamine, or vehicle for 24 h in DMEM with 0.5% FBS. *B*, effect of PTX treatment in Ptc1$^{+/-}$ cells was also quantified by real-time PCR. *C*, effect of PTX, KAAD-cyclopamine, and LY294002 on the basal expression level of *gli1* in Ptc1$^{-/-}$ and SMO$^{-/-}$ cells. *D*, expression of Gα_z in membranes isolated from Ptc1$^{+/-}$ MEFs or platelets (positive control) by Western blot.

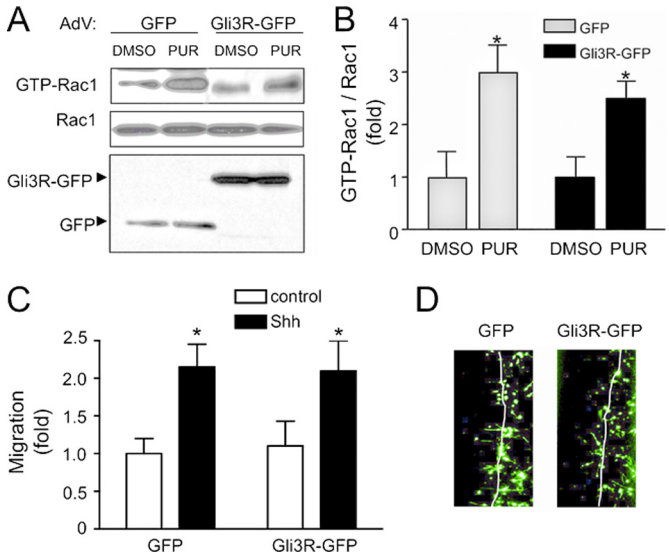

FIGURE 8. **SMO-mediated Rac1 activation is independent of Gli transcriptional activity.** *A*, Ptc1$^{+/-}$ MEFs were transduced with control GFP-AdV or Gli3R-GFP-AdV (MOI = 150). Following 24 h of serum starvation, cells were stimulated with 5 μM purmorphamine (*PUR*) or vehicle (DMSO) for 5 min, and GTP-Rac1 levels were determined by pulldown assays. Expression of the transgenes was confirmed by Western blot against GFP. *B*, quantification of GTP-Rac1 activation by purmorphamine in the presence of Gli3R or GFP (n = 3). *, $p < 0.05$. *C*, quantification of wound healing assays of Ptc1$^{+/-}$ MEFs transduced with GFP-AdV or Gli3R-GFP-AdV and stimulated at $t = 0$ with 2.5 μg/ml Shh or vehicle. Values represent the fold increase of GFP$^+$ cells that migrate into the wound; *, $p < 0.05$. *D*, representative images of migration of cells expressing GFP or Gli3R-GFP after 8 h in the presence of Shh. The *white line* shows the scratch border at $t = 0$.

significant levels of G_z. PTX catalyzes the ADP-ribosylation of the Gα subunits of all G_i family members with the exception of Gα_z. However, Gα_z was barely, if at all, detectable in MEFs by Western blot of total membrane fractions (Fig. 7*D*). The very low levels of G_z plus the almost complete sensitivity of events underlying migration to PTX as a control for the efficacy of the toxin attest to the fact that G_i function is not required for the activation of Gli in MEFs.

To more firmly establish that migration and activation of Rho and Rac by Shh is independent of the canonical (Gli) pathway in MEFs, we inhibited Gli-mediated transcription with a GFP fusion of Gli3R, which competes at the promoter regions for Gli-binding sites and acts as a strong repressor of Gli transcription (28). Ptc1$^{+/-}$ MEFs were infected with Gli3R-GFP AdV or GFP AdV (control), serum-starved overnight, and exposed the following day to vehicle or purmorphamine for 5 min. Rac pulldown assays showed that neither expression of Gli3R-GFP nor GFP alone impaired Rac activation by purmorphamine (Fig. 8, *A* and *B*). In addition, expression of Gli3R did not perturb Shh-induced fibroblast migration (Fig. 8, *C* and *D*). These data confirm that the rapid effects of Shh on cell motility through engagement of small GTPases are independent of Gli transcriptional activity.

SMO Variants Rescue Activation of Rac and Rho in SMO-null Fibroblasts Irrespectively of Canonical Hh Pathway—For activation of the canonical, Gli-dependent pathway, SMO undergoes translocation to the primary cilium of cells, a single organelle transiently formed during interphase by both lateral plasma membrane diffusion and by fusion of intracellular SMO-containing vesicles. Translocation of SMO is promoted by purmorphamine and other SMO synthetic agonists and is prevented by Ptc1. Ciliary localization of SMO requires a two-residue motif at the beginning of the intracellular C-terminal tail. The C-terminal tail is an essential domain for β-arrestin recruitment and interaction with Suppressor of Fused, both prerequisites for Gli activation, but is dispensable for coupling to heterotrimeric G_i proteins (14, 29, 30). To evaluate whether migration of fibroblasts and activation of the small GTPases Rac1 and RhoA in response to Shh are independent of the canonical Hh pathway, we introduced different SMO variants into SMO$^{-/-}$ MEFs to evaluate which domain of SMO can rescue the defects in migration and small GTPase activation. We generated stable SMO-null transfectants harboring empty plasmid, SMO-M2 (W535L), which is constitutively active toward both G_i and the Gli activation pathway, SMO-M2-CLD (W535L,W549A,R550A), which is reported to be ciliary localization-deficient (31), and SMO-M2-ΔC (SMO-1–551,W535L), which activates G_i but is unable to activate Gli (14). Using an antibody directed toward the C-terminal region of SMO (including the seventh transmembrane domain), we verified expression of SMO-M2 and SMO-M2-CLD in geneticin-resistant cells and a weaker expression of SMO-M2-ΔC (Fig. 9*A*). Expression of Gli target genes was restored in MEFs expressing SMO-M2, as expected, but not in those expressing SMO-M2-ΔC (Fig. 9*B*). Unexpectedly, *gli1* expression was also restored in MEFs expressing the ciliary localization-deficient SMO variant, in apparent contrast with a recent publication (31). All three SMO-M2 variants, and most remarkably SMO-M2-ΔC, were able to rescue the activation of Rac1 and RhoA irrespective of their ability to activate the canonical pathway (Fig. 8, *B* and *C*). Finally, we found that basal migration rate in wound healing assays was increased significantly in SMO$^{-/-}$ MEFs stably expressing all three SMO-M2

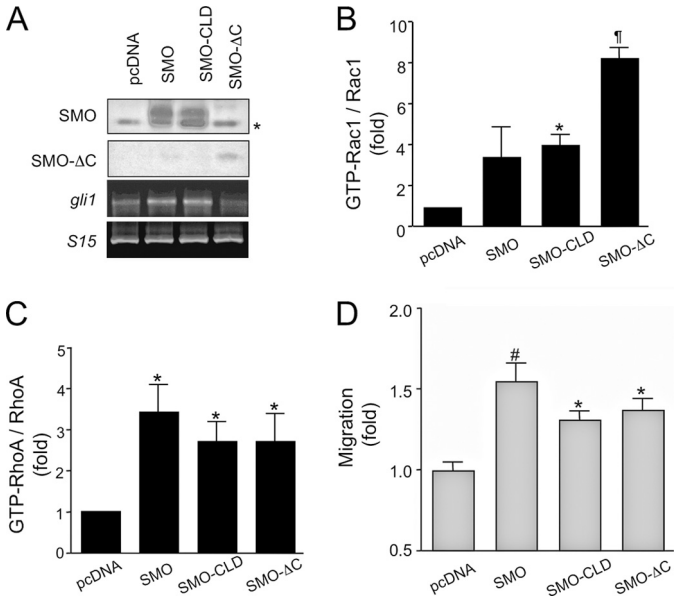

FIGURE 9. **SMO promotes monomeric GTPase activation and cell migration independently of its capacity to induce *gli1*.** *A*, *upper gels*, expression of SMO variants in membranes prepared from $SMO^{-/-}$ MEFs stably transfected with empty pcDNA3.1vector (pcDNA), SMO-M2 (SMO), SMO-M2-CLD (SMO-CLD), or SMO-M2-ΔC (SMO-ΔC) was assessed by Western blot with anti-SMO E5 mAb. Full-length SMO variants run at ~90 kDa, whereas SMO-ΔC runs at ~55 kDa. The *asterisk* marks a cross-reactive band. *Bottom* gels, expression of *gli1* and *S15* in the same cell lines was determined by semiquantitative RT-PCR after 24 h of serum starvation at high cell density. *B*, densitometry values of Rac1 activation of the indicated cell lines after 5 min of stimulation with 5 μM purmorphamine ($n = 3$; *, $p < 0.05$; ¶, $p < 0.01$). *C*, densitometry values of RhoA activation of the indicated cell lines after 5 min of stimulation with 5 μM purmorphamine ($n = 3$; *, $p < 0.05$). *D*, purmorphamine-induced migration (fold compared with DMSO) of $SMO^{-/-}$ fibroblasts containing empty vector or the three SMO-M2 variants ($n = 3$). #, $p < 0.01$; *, $p < 0.05$.

variants (Fig. 8*D*). The results with SMO-M2-ΔC demonstrate again the capacity of SMO to activate events underlying migration in a fashion independent of Gli.

DISCUSSION

The function of SMO as a G protein-coupled receptor, often overlooked in view of what many perceive as a G protein-independent engagement of Gli transcription factors, is central for activation of Rho family GTPases by Shh and, consequently, for Shh-dependent migration of fibroblasts. The present study underscores a duality in transduction, wherein the activation of Rho GTPases and stimulation of migration occur through G_i and are independent of the engagement of Gli. The requirement for SMO in the actions of Shh is based on (*i*) the pro-migratory actions of purmorphamine, an agonist working directly on Smo, (*ii*) enhanced migration of $Ptc^{-/-}$ MEFs that is sensitive to KAAD-cyclopamine, and (*iii*) impaired migration in $SMO^{-/-}$ MEFs. The requirement for G_i is based on sensitivity of migration to PTX. In this regard, we note that both wild-type and truncated forms of SMO couple strongly and selectively to this family of G proteins (14). The requirement for signaling apart from Gli is based on the activity of a SMO mutant devoid of the C-terminal tail and the inactivity of a repressor of Gli signaling toward migration.

We extended our previous studies (18) to confirm that not only is RhoA a target for Smo through G_i, but that the activation proceeds through Rac1 in a hierarchal fashion and that both of the monomeric G proteins underlie migration. It has been documented previously in Swiss 3T3 fibroblasts that microinjection of a mutant active Rac1V12 stimulates actin polymerization with formation of membrane ruffles first, and after 20–30 min induces Rho-dependent formation of stress fibers (32). Moreover, inhibition of Rac function by expression of dominant negative RacN17 blocks activation of RhoA induced by several growth factors, including PDGF, EGF, and insulin (32, 33). Our findings that RhoA activation is dependent on Rac1 activity are in line with these observations. Those same growth factors activate Rac and Rho through a mechanism dependent on PI3K activity, as assessed by sensitivity to wortmannin (33). These growth factors act on tyrosine kinase receptors, the agonists used here (Shh and purmorphamine) however act on a 7-TM receptor. In this regard, lysophosphatidic acid and bombesin, also acting on 7-TM receptors, activate Rac1 through G_i/PI3K (33) and RhoA through G_{13}/RhoGEFs (reviewed in Ref. 34) in fibroblasts. SMO is unable to couple directly to G_{13} (14); thus, the stimulation of RhoA by SMO can be explained only by a hierarchal G_i/PI3K/Rac1 series of activations; the activation of RhoA by Rac1 could conceivably be related to transactivation of a G_{13}-coupled receptor. Despite the rarity of G_i-mediated activation of RhoA in the literature, this is not completely unprecedented because stimulation of muscarinic receptors by carbachol results in Rho activation and stress fiber formation in a pertussis toxin-sensitive manner (35).

It would seem that Hh signaling diverges at the level of SMO into transcriptional and non-transcriptional, cytoskeletal pathways, akin to signaling achieved by the Frizzled receptors for Wnt isoforms. In Wnt signaling, different pairs of ligand/receptor engage either the canonical β-catenin pathway (transcriptional) or the planar polarity (cytoskeletal) pathway in a cell type-specific fashion (36, 37). Not surprisingly, Frizzled receptors and SMO are sole members of a subfamily among the G protein coupled receptor superfamily (38), and Frizzled has also been shown to couple to the G_i protein family, specifically to G_o (39). This unprecedented parallel perhaps exposes a conservation of functions related by the structure of these atypical G protein coupled receptors.

The function and localization of SMO is regulated by specific regions of the protein; a mutant of SMO lacking the C-terminal tail retains the ability to couple to G_i, indicating that the intracellular loops of SMO mediate interaction with G_i, as is the case for most G protein coupled receptors (40). Indeed, this mutant couples more efficiently with G_{i2} than the full-length protein (14), suggesting a partial steric inhibition by the C-terminal tail. The form of SMO lacking the C-terminal tail is, however, unable to engage the pathway targeting Gli. The C-terminal tail, therefore is required for canonical signaling, yet it, too, is insufficient in this regard (14, 30). Clearly, two or more elements of SMO structure are relevant to the canonical pathway. In the case of NIH 3T3 fibroblasts, zebrafish embryos (41) and the *Drosophila* wing imaginal disc (42), one of these elements is coupling to G_i. In some cells, for example MEFs, G_i is not required. We believe the requirement for G_i as it pertains to Gli activation can be superceded in some cells by other forms of signaling perhaps unrelated to SMO.

Our results with SMO lacking the C-terminal tail clearly indicate that the C-terminal tail is not required for RhoA and Rac1 activation, as it is not required for heterotrimeric G_i proteins. These results suggest that regulation of the cell motility is a prototypical non-canonical response to Shh. We also tested whether a two residue mutation of SMO (W549A,R550A) that purportedly prevents translocation to the primary cilium, and therefore cannot activate Gli, could restore a migratory response to SMO-deficient cells. As expected, the mutation on a constitutively active SMO background (SMO-M2-CLD) rescued the phenotype, but it also induced activation of Gli. We do not know the reason for the discrepancy in our results in relation to those published, but we believe that the active conformation of SMO-M2 can perhaps promote ciliary localization independently of the WR motif, perhaps due to β-arrestin2 binding.

In summary, our findings underscore non-canonical signaling of SMO through G_i and monomeric G proteins as an important facet of Hh signaling. Our data are limited to migration; however, a number of events documented for Hh signaling occur in a time frame that all but precludes transcription as a basis. These include not only fibroblast migration but also axon guidance, endothelial tubulogenesis, and reduction of caspase activation by growth factor withdrawal (17–19). To what extent any of these are under the control of G_i remains to be documented. The emerging parallels between SMO and Frizzled proteins, as well, may help inform the activities under control of the non-canonical pathway.

Acknowledgments—We thank Matthew Scott and James Chen (Stanford University), Marcelo Kazanietz (University of Pennsylvania), Bradley Yoder (University of Alabama), and Andrew Aplin and Wally Koch (Thomas Jefferson University) for providing us with valuable reagents and Feng Shen (University of Pennsylvania) for technical assistance.

REFERENCES

1. Riobo, N. A., and Manning, D. R. (2007) *Biochem. J.* **403,** 369–379
2. Ruiz i Altaba, A., Sánchez, P., and Dahmane, N. (2002) *Nat. Rev. Cancer.* **2,** 361–372
3. McMahon, A. P., Ingham, P. W., and Tabin, C. J. (2003) *Curr. Top. Dev. Biol.* **53,** 1–114
4. Yang, L., Xie, G., Fan, Q., and Xie, J. (2010) *Oncogene* **29,** 469–481
5. Scales, S. J., and de Sauvage, F. J. (2009) *Trends Pharmacol. Sci.* **30,** 303–312
6. Nakamura, K., Sasajima, J., Mizukami, Y., Sugiyama, Y., Yamazaki, M., Fujii, R., Kawamoto, T., Koizumi, K., Sato, K., Fujiya, M., Sasaki, K., Tanno, S., Okumura, T., Shimizu, N., Kawabe, J., Karasaki, H., Kono, T., Ii, M., Bardeesy, N., Chung, D. C., and Kohgo, Y. (2010) *PLoS One* **5,** e8824
7. Theunissen, J. W., and de Sauvage, F. J. (2009) *Cancer Res.* **69,** 6007–6010
8. Tian, H., Callahan, C. A., DuPree, K. J., Darbonne, W. C., Ahn, C. P., Scales, S. J., and de Sauvage, F. J. (2009) *Proc. Natl. Acad. Sci. U.S.A.* **106,** 4254–4259
9. Rohatgi, R., Milenkovic, L., and Scott, M. P. (2007) *Science* **317,** 372–376
10. Seeley, E. S., and Nachury, M. V. (2010) *J. Cell Sci.* **123,** 511–518
11. Milenkovic, L., Scott, M. P., and Rohatgi, R. (2009) *J. Cell Biol.* **187,** 365–374
12. Wang, Y., Zhou, Z., Walsh, C. T., and McMahon, A. P. (2009) *Proc. Natl. Acad. Sci. U.S.A.* **106,** 2623–2628
13. Kim, J., Kato, M., and Beachy, P. A. (2009) *Proc. Natl. Acad. Sci. U.S.A.* **106,** 21666–21671
14. Riobo, N. A., Saucy, B., Dilizio, C., and Manning, D. R. (2006) *Proc. Natl. Acad. Sci. U.S.A.* **103,** 12607–12612
15. Low, W. C., Wang, C., Pan, Y., Huang, X. Y., Chen, J. K., and Wang, B. (2008) *Dev. Biol.* **321,** 188–196
16. Jenkins, D. (2009) *Cell Signal* **21,** 1023–1034
17. Lipinski, R. J., Bijlsma, M. F., Gipp, J. J., Podhaizer, D. J., and Bushman, W. (2008) *BMC Cell Biol.* **9,** 49
18. Chinchilla, P., Xiao, L., Kazanietz, M. G., and Riobo, N. A. (2010) *Cell Cycle* **9,** 570–579
19. Yam, P. T., Langlois, S. D., Morin, S., and Charron, F. (2009) *Neuron* **62,** 349–362
20. Martinez-Chinchilla, P., and Riobo, N. A. (2008) *Methods Enzymol.* **446,** 189–204
21. Yang, C., Liu, Y., Leskow, F. C., Weaver, V. M., and Kazanietz, M. G. (2005) *J. Biol. Chem.* **280,** 24363–24370
22. Ren, X. D., and Schwartz, M. A. (2000) *Methods Enzymol.* **325,** 264–272
23. Bailey, E. C., Milenkovic, L., Scott, M. P., Collawn, J. F., and Johnson, R. L. (2002) *J. Biol. Chem.* **277,** 33632–33640
24. Woodard, A. S., García-Cardeña, G., Leong, M., Madri, J. A., Sessa, W. C., and Languino, L. R. (1998) *J. Cell Sci.* **111,** 469–478
25. Milenkovic, L., Goodrich, L. V., Higgins, K. M., and Scott, M. P. (1999) *Development* **126,** 4431–4440
26. Riobó, N. A., Lu, K., Ai, X., Haines, G. M., and Emerson, C. P., Jr. (2006) *Proc. Natl. Acad. Sci. U.S.A.* **103,** 4505–4510
27. Stecca, B., and Ruiz I Altaba, A. (2010) *J. Mol. Cell. Biol.* **2,** 84–95
28. Meyer, N. P., and Roelink, H. (2003) *Dev. Biol.* **257,** 343–355
29. Chen, W., Ren, X. R., Nelson, C. D., Barak, L. S., Chen, J. K., Beachy, P. A., de Sauvage, F., and Lefkowitz, R. J. (2004) *Science* **306,** 2257–2260
30. Varjosalo, M., Li, S. P., and Taipale, J. (2006) *Dev. Cell.* **10,** 177–186
31. Corbit, K. C., Aanstad, P., Singla, V., Norman, A. R., Stainier, D. Y., and Reiter, J. F. (2005) *Nature* **437,** 1018–1021
32. Ridley, A. J., Paterson, H. F., Johnston, C. L., Diekmann, D., and Hall, A. (1992) *Cell* **70,** 401–410
33. Nobes, C. D., Hawkins, P., Stephens, L., and Hall, A. (1995) *J. Cell Sci.* **108,** 225–233
34. Riobo, N. A., and Manning, D. R. (2005) *Trends Pharmacol. Sci.* **26,** 146–154
35. Togashi, H., Emala, C. W., Hall, I. P., and Hirshman, C. A. (1998) *Am. J. Physiol.* **274,** 803–809
36. Widelitz, R. (2005) *Growth Factors* **23,** 111–116
37. Rao, T. P., and Kühl, M. (2010) *Circ. Res.* **106,** 1798–1806
38. Kristiansen, K. (2004) *Pharmacol. Ther.* **103,** 21–80
39. Katanaev, V. L., Ponzielli, R., Sémériva, M., and Tomlinson, A. (2005) *Cell* **120,** 111–122
40. Fanelli, F., De Benedetti, P. G., Raimondi, F., and Seeber, M. (2009) *Curr. Protein Pept. Sci.* **10,** 173–185
41. Hammerschmidt, M., and McMahon, A. P. (1998) *Dev. Biol.* **194,** 166–171
42. Ogden, S. K., Fei, D. L., Schilling, N. S., Ahmed, Y. F., Hwa, J., and Robbins, D. J. (2008) *Nature* **456,** 967–970